# Chaotic advection, diffusion, and reactions in open flows

Tamás Tél
*Institute for Theoretical Physics, Eötvös University, P.O. Box 32, H-1518 Budapest, Hungary*

György Károlyi
*Department of Civil Engineering Mechanics, Technical University of Budapest, Müegyetem rpk. 3, H-1521 Budapest, Hungary*

Áron Péntek
*Marine Physical Laboratory, Scripps Institution of Oceanography, University of California at San Diego, La Jolla, California 92093-0238*

István Scheuring
*Department of Plant Taxonomy and Ecology, Research Group of Ecology and Theoretical Biology, Eötvös University, Ludovika tér 2, H-1083 Budapest, Hungary*

Zoltán Toroczkai
*Department of Physics, University of Maryland, College Park, Maryland 20742-4111 and Department of Physics, Virginia Polytechnic Institute and State University, Blacksburg, Virginia 24061-0435*

Celso Grebogi
*Institute for Plasma Research, University of Maryland, College Park, Maryland 20742*

James Kadtke
*Marine Physical Laboratory, Scripps Institution of Oceanography, University of California at San Diego, La Jolla, California 92093-0238*

We review and generalize recent results on advection of particles in open time-periodic hydrodynamical flows. First, the problem of passive advection is considered, and its fractal and chaotic nature is pointed out. Next, we study the effect of weak molecular diffusion or randomness of the flow. Finally, we investigate the influence of passive advection on chemical or biological activity superimposed on open flows. The nondiffusive approach is shown to carry some features of a weak diffusion, due to the finiteness of the reaction range or reaction velocity. © *2000 American Institute of Physics.* [S1054-1500(00)02001-2]

Advection of passive tracers in open nonstationary flows is an interesting phenomenon because even in simple time-periodic velocity fields the tracer particles can exhibit chaotic motion, and tracer ensembles display pronounced fractal patterns. As an illustrative numerical experiment we analyze a model of the von Kármán vortex street, a time-periodic two-dimensional flow of a viscous fluid around a cylinder. First, we consider the problem of passive advection, and discuss the chaoticity of the particle dynamics and its relationship to the appearance of fractal patterns. Then we include weak diffusion and show that this leads to a washing out of the fine-scale structure below a critical length scale, while still preserving fractal scaling above this scale. Finally, we study how chemical or biological processes superimposed on open flows are influenced by the properties of the underlying nondiffusive passive advection. We present an elementary derivation of the reaction equation that describes accumulation of products along the unstable manifold. Moreover, the similarity of this fattening of a fractal to that due to diffusion is discussed and analyzed, and our method is compared with the traditional description via reaction-advection-diffusion equations.

## I. PASSIVE ADVECTION IN OPEN FLOWS

The advection of particles by hydrodynamical flows has attracted recent interest from the dynamical system community.[1–32]

If advected particles take on the velocity of the flow very rapidly, i.e., inertial effects are negligible, we call the advection passive and the particle a passive tracer. The equation for the position $\mathbf{r}(t)$ of the particle is then

$$\dot{\mathbf{r}} = \mathbf{v}(\mathbf{r}, t), \tag{1}$$

where $\mathbf{v}$ represents the velocity field that is assumed to be known. The tracer dynamics is thus governed by a set of ordinary differential equations, e.g., like those of a driven anharmonic oscillator, whose solution is typically chaotic.

A unique feature of chaotic advection in time-dependent *planar incompressible* flows is that the fractal structures characterizing chaos in phase space become observable by the naked eye in the form of spatial patterns.[1–4] In such cases there exists a *streamfunction* $\psi_{\mu(t)}(x, y)$ (Ref. 33) whose derivatives can be identified with the velocity components as

$$v_x(x, y, t) = \frac{\partial \psi_{\mu(t)}(x, y)}{\partial y}, \quad v_y(x, y, t) = -\frac{\partial \psi_{\mu(t)}(x, y)}{\partial x}, \tag{2}$$

and whose level curves provide the streamlines. The subscript $\mu(t)$ indicates the set of all parameters determining the streamfunction, which is generally time dependent. Note that Eq. (2) is a consequence of incompressibility because it implies $\nabla \cdot \mathbf{v} = 0$. Combining Eq. (2) with Eq. (1) for a planar flow, where $\mathbf{r} = (x,y)$ and $\mathbf{v} = (v_x, v_y)$, one notices that the equations of motion have canonical character, with $\psi_{\mu(t)}(x,y)$ playing the role of the Hamiltonian and $x$ and $y$ being the canonical coordinates and momenta (or vice versa), respectively. Thus, the plane of the flow *coincides* with the particles' phase space. This property makes passive advection in planar incompressible flows especially interesting and a good candidate for an experimental observation of patterns that are typically hidden in an abstract phase space. In stationary flows when $\psi$ is independent of $t$, the system (1) and (2) is integrable and the particle trajectories coincide with the streamlines. In time-dependent cases, however, particle trajectories and streamlines are different, and the former ones can only be obtained by solving Eqs. (1) and (2) numerically.

Here we consider passive advection in *open* flows. This means that there is a net current flowing through the observation region where the velocity field is time dependent. In the far upstream and far downstream regions the flow is considered stationary. In such cases complicated tracer movements are restricted to a *finite* region. This will be called the *mixing region* outside of which the time dependence of $\psi$ is negligible. It is worth emphasizing that a complicated flow field (turbulence) inside the mixing region is *not* required for a complex tracer dynamics or for the appearance of fractal patterns. Even simple forms of time dependence, e.g., a periodic repetition of the velocity field with some period $T$, is sufficient. However, the periodicity of such flows allows for a simpler presentation of the chaotic advection dynamics via the so-called stroboscopic map. It is a discrete map $M_\mu$ defined by the sequence of snapshots taken at time instants separated by $T$ connecting the coordinates $(x_n, y_n)$ of the particle at snapshot $n$ with those at the next one as

$$(x_{n+1}, y_{n+1}) = M_\mu(x_n, y_n). \tag{3}$$

Since the parameters of the flow are time periodic with $T$, the parameters $\mu$ on the snapshots are $n$-independent, and hence the map is autonomous. Due to the incompressibility of the flow, map $M_\mu$ is area preserving.

The complicated form of trajectories implies a long time spent in the mixing region. In other words, tracers can be temporarily trapped there. It is even more surprising, however, that for very special initial tracer positions *nonescaping orbits* exist. The simplest among these orbits are the periodic ones with periods that are integer multiples of the flow's period, $T$. All the nonescaping orbits are highly unstable and possess a strictly positive local Lyapunov exponent. Another important feature of these orbits is that they are rather exceptional so that they cannot fill a finite portion of the plane. Indeed, the union of all nonescaping orbits forms a fractal cloud of points on a stroboscopic map. This cloud is moving periodically with the flow but never leaves the mixing region.

Typical tracer trajectories not exactly reaching any of the nonescaping orbits are, however, influenced by them. They follow some of the periodic orbits for awhile and later turn to follow another one. This wandering among periodic (or, more generally, nonescaping) orbits results in the *chaotic motion* of passive tracers. Indeed, as long as the tracers are in the mixing region, their trajectories possess a positive average Lyapunov exponent $\lambda$. Hence the union of all nonescaping orbits is called the *chaotic saddle*. It has a unique fractal dimension $D_0^{(\text{saddle})}$ on a stroboscopic map, independent of the time instant at which the snapshot is taken.

While many of the tracers spend a long time in the mixing region, the overwhelming majority of particles leaves this region sooner or later. The decay of their number in a fixed frame is typically exponential with a positive exponent $\kappa \, (<\lambda)$, which is independent of the frame. This quantity is the *escape rate* from the saddle (or the mixing region). The reciprocal of the escape rate can also be considered as the average lifetime of chaos, and therefore the chaotic advection of passive tracers in open flows is *transient chaos*.[34]

The chaotic saddle is the set of nonescaping orbits which tracer particles can follow for an arbitrarily long time. Each orbit of the set, and therefore the set as a whole, has a stable and an unstable *manifold*. The *stable* manifold is a set of points along which the saddle can be reached after an infinitely long time. The *unstable* manifold is the set along which particles lying infinitesimally close to the saddle will eventually leave it in the course of time. Viewed on a stroboscopic map, these manifolds are *fractal curves*, winding in a complicated manner. By looking at different snapshots of these curves we can observe that they move periodically with the period $T$ of the flow. Their fractal dimension $D_0$ ($1 < D_0 < 2$) is, however, independent of the snapshot. [The stable and unstable manifolds have identical fractal dimension due to the tracer dynamics' time reversal invariance, and $D_0^{(\text{saddle})} = 2(D_0 - 1)$.]

The unstable manifold plays a special role since it is the only manifold which can be directly observed in an experiment. Let us consider a droplet (ensemble) of a large number of particles which initially overlaps with the stable manifold. As the droplet is advected into the mixing region its shape is strongly deformed, but the ensemble comes closer and closer to the chaotic saddle as time goes on. Since, however, only a small portion of particles can fall very close to the stable manifold, the majority do not reach the saddle and start flowing away from it along the unstable manifold. Therefore we conclude that in open flows *droplets of particles trace out the unstable manifold* of the chaotic saddle after a sufficiently long time of observation. This implies that classical flow visualization techniques based on dye evaporation or streaklines trace out fractal curves (unstable manifolds) which are *different from streamlines* or any other characteristics of the Eulerian velocity field (for several flow visualization photographs of this type, see Ref. 35).

A classical result, valid for any transient chaotic motion, relates the dynamical quantities to the fractality of the manifolds.[36,34,37] Applied to our particular problem, it implies that the information dimension $D_1$ of the manifold is uniquely related to the average Lyapunov exponent $\lambda$ around the chaotic saddle and the escape rate $\kappa$:

$$D_1 = 2 - \frac{\kappa}{\lambda}. \tag{4}$$

This formula says that the unstable manifold's dimension is smaller than the plane's dimension by an amount given by the ratio $\kappa/\lambda$ of two dynamical rates, or two characteristic times. Since the fractal dimension $D_0$ of the manifold is typically very close (from above) to $D_1$, Eq. (4) also provides a fairly good estimate of $D_0$.

The derivation of Eq. (4) is based on the observation that if we cover the unstable manifold in a given region with boxes of linear size $\epsilon$ and color the covered area $\mathcal{A}$, the colored area $\mathcal{A}'$ staying inside the preselected region after some time $\tau$ will be smaller by a factor of $\exp(-\kappa\tau)$ due to escape. Simultaneously, the covering will be narrower due to the convergence along the stable direction towards the unstable manifold. Therefore we write that the new box size is $\epsilon' = \epsilon \exp(-\lambda\tau)$ where $-\lambda$ is the average negative Lyapunov exponent. By this we are considering boxes which are *typical* with respect to the natural measure[34] on the saddle and so their number $N(\epsilon)$ scales as $\epsilon^{-D_1}$. This exponent $D_1$ is somewhat smaller than the fractal dimension determining the scaling of all the covering boxes. Since, however, our boxes are typical, the total covered area is $\mathcal{A} \sim \epsilon^{2-D_1}$ and $\mathcal{A}' \sim \epsilon'^{2-D_1}$ up to corrections which are negligible in the small $\epsilon$ limit. By inserting the relation between the box sizes and the areas, we find that Eq. (4) holds irrespective of $\tau$.

It is worth emphasizing the usefulness of a further, independent characteristic, the *topological entropy* $K_0$ of the chaotic saddle. It can be interpreted[25,11,38] as the growth rate of the length $L(t)$ of material lines or of the droplet perimeters in a fixed region of observation as a function of time $t$:

$$L(t) \sim e^{K_0 t} \tag{5}$$

for asymptotically long times. In spite of the very natural measurability of these lengths in passive advection, the use of topological entropy is not yet widespread. The quantity $K_0$ provides an upper bound to the metric entropy $K_1$ which turns out to be the difference between the Lyapunov exponent and the escape rate:[36,34]

$$K_0 \geqslant K_1 = \lambda - \kappa. \tag{6}$$

The average Lyapunov exponent can also be expressed as the average growth rate of $\ln L(t)$ around the chaotic saddle. The difference between $K_0$ and $\lambda$ is due to the difference between the logarithm of an average and the average of a logarithm.

Next, as a paradigm of two-dimensional viscous flows around obstacles, we consider the case of the particle motion around a cylinder. We work in a range of parameters where a von Kármán vortex street exists, and vortices are detaching from the upper and lower halves of the cylinder with a period $T$. Experiments carried out in this flow proved the existence of unstable periodic orbits and of a fractal unstable manifold.[39] This problem has also been investigated numerically in great detail.[21–25] For simplicity we take an analytical model for the streamfunction introduced in Ref. 24. It describes the flow when only two vortices are present in the

wake of the cylinder at any instant of time and these vortices alternate when separating from the cylinder. The form of the analytical model is motivated by the results of a direct numerical simulation of the Navier–Stokes equations at Reynolds number 250, reported in Ref. 23. The dynamical and geometrical parameters $\lambda, \kappa, K_0$, and $D_0$ are functions of the Reynolds number. The wake of the cylinder plays the role of the mixing region.

It is worth emphasizing that relations (4) and (6) are valid for hyperbolic chaotic saddles only. The chaotic saddles in advection problems typically also contain nonhyperbolic components. One source of them can be KAM tori generated by the Hamiltonian problem (1) and (2).[10–12,14,15,26] In the wake of the cylinder, however, they can hardly be observed.[24,39] The applied resolutions suggest that they are certainly not present on dimensionless length scales above $10^{-4}$. Another, independent source is the surface of the cylinder. It acts as a union of parabolic orbits, and hence as a smooth torus, which is also sticky. Close to the surface, i.e., in the boundary layer, this stickiness leads to an immediate power law decay,[24] but further out in the wake exponential decay can be observed over more than 15 periods. Thus, the advection problem in the wake can faithfully be described over a long time span as if the saddle was fully hyperbolic. Thus, (4) and (6) can safely be used in this context.

Figure 1 displays the unstable manifold of the chaotic saddle taken at different snapshots within one period. The radius $R$ of the cylinder and the period $T$ of the flow are taken as the length and time units. The construction is based on the mathematical definition of the unstable manifolds, therefore what we see are infinitesimally thin lines. As a comparison, Fig. 2 illustrates the droplet dynamics mentioned above. It shows the shape of an originally compact droplet as time goes on. We can observe that after a sufficiently long time the droplet traces out the unstable manifold. Due to the finite number of particles, however, the chaotic saddle cannot be reached exactly, and the number of particles in the wake tends to zero in the long time limit. Permanent fractal patterns can only be observed if there is a continuous inflow of tracers in front of the cylinder.

## II. DIFFUSION AND RANDOM FLOWS

The effect of molecular diffusion on passive advection can be taken into account by considering, instead of Eqs. (1) and (2), their stochastic counterparts augmented by Langevin terms:[3,17]

$$\dot{x} = \frac{\partial \psi_{\mu(t)}(x,y)}{\partial y} + \xi_x(t), \quad \dot{y} = -\frac{\partial \psi_{\mu(t)}(x,y)}{\partial x} + \xi_y(t). \tag{7}$$

Here $\xi_x$, $\xi_y$ represent, in the simplest case, uncorrelated, Gaussian noises with white autocorrelation functions:

$$\langle \xi_x(t)\xi_x(t') \rangle = 2D\delta(t-t'), \tag{8}$$

$$\langle \xi_y(t)\xi_y(t') \rangle = 2D\delta(t-t'), \tag{9}$$

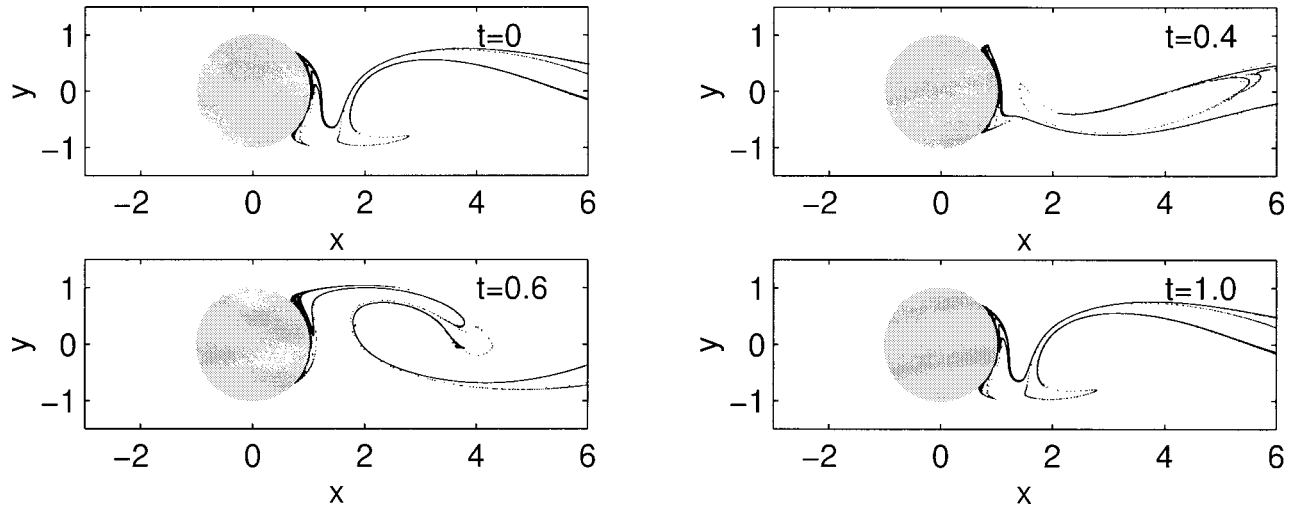where $D$ is the molecular diffusion coefficient and is assumed to be isotropic in the plane.

FIG. 1. Snapshots taken on the unstable manifold of the chaotic saddle at times $t=0,\frac{2}{5},\frac{3}{5}$, and 1 in the wake of the cylinder. This fractal pattern is time periodic with the period of the flow. $t=0$ is the instant when a vortex is born close to the first quadrant of the cylinder surface. The length is measured in units of cylinder radius $R$.

In the case of time-periodic flows this leads to a noisy stroboscopic map taken with the period $T$ of the flow

$$(x_{n+1},y_{n+1})=M_{\mu}(x_n,y_n)+(\xi_{x,n},\xi_{y,n}), \tag{10}$$

where the noise terms $\xi_{x,n},\xi_{y,n}$ obey similar characteristics as their continuous counterparts. The autonomous property of the map is broken due to the appearance of additive noise: the full map depends on the snapshot taken, i.e., on $n$. Furthermore, it is no longer exactly area preserving.

Let us now qualitatively formulate how molecular diffusion modifies the behavior around the filaments of the unstable manifold, assuming the case of weak diffusion. One then expects to see diffusive effects on small scales only. This implies that the convergence of a droplet towards the unstable manifold can be observed similarly as without diffusion, but not up to infinite accuracy. If a filament is locally covered by particles in a sufficiently narrow band of width $\delta$, this width can change in time due to two *competing* effects. It tends to broaden because of diffusion, but also shrinks because of the contraction along the stable direction, i.e., perpendicular to the filament. These effects result in a certain time dependence of $\delta$ which leads to a *steady state* in which the two effects exactly compensate each other.

To see this qualitatively, let us follow the evolution of the filament width $\delta_n$ over a time interval $\tau$. It increases to $(\delta_n^2+2D\tau)^{1/2}$ according to the usual spreading due to diffusion, multiplied by the typical shrinking factor $\exp(-\lambda\tau)$. So all together the new width is

$$\delta_{n+1}=(\delta_n^2+2D\tau)^{1/2}e^{-\lambda\tau}. \tag{11}$$

This equation has obvious steady solutions. By requiring that $\delta'=\delta\equiv\delta^*$ we find

$$\delta^*=\left(\frac{2D\tau}{e^{2\lambda\tau}-1}\right)^{1/2}. \tag{12}$$

This describes a solution in which the coverage of the filaments by tracers is changing in time in a periodic fashion

corresponding to a limit cycle behavior repeating itself after time intervals $\tau$. The flow in the wake of the cylinder is time periodic with $T$ but, since it is reflection symmetric with respect to the $x$-axis after a time shift of $T/2$, we expect a steady solution for the diffusive case with $\tau=T/2$.

The solution is simpler if $\lambda\tau\ll1$, formally corresponding to the limit $\tau,T\rightarrow0$, since then

$$\delta^*=\left(\frac{D}{\lambda}\right)^{1/2}. \tag{13}$$

The asymptotic solution is then strictly constant in time, and appears to be a fixed point of the $\delta$-dynamics. This formula can be used as a first guess for the filament width even for finite values of $\tau$ since Eq. (12) can be written as $\sqrt{D/\lambda}$ multiplied by a dimensionless function of $\lambda\tau$. Both cases illustrate that the coverage of the manifold's filaments follows a dissipative $\delta$-dynamics, in spite of the Hamiltonian character of the original passive advection problem [Eqs. (1) and (2)]. This dynamics can also be expressed in terms of a differential equation in the limit $\tau\rightarrow0$:

$$\dot{\delta}=\frac{D}{\delta}-\lambda\delta, \tag{14}$$

which has (13) as its steady-state solution. Irrespective of the form of the advection dynamics, we conclude that in the presence of diffusion, the fractal scaling of the asymptotic tracer distribution remains valid beyond the crossover distance $\delta^*$ with the same dimensions $D_0$ or $D_1$ as without diffusion, but below $\delta^*$ the distribution is smoothed out.

One can also estimate the time $t_d$ needed to see the effect of diffusion. Starting with a droplet of linear size of order unity, the typical width of its filaments decreases as $\exp(-\lambda t)$. At $t_d$ it reaches the size of $\sqrt{D/\lambda}$ which yields $t_d\sim1/\lambda\ln D$, i.e., the diffusion time depends logarithmically on the magnitude of the diffusion coefficient.

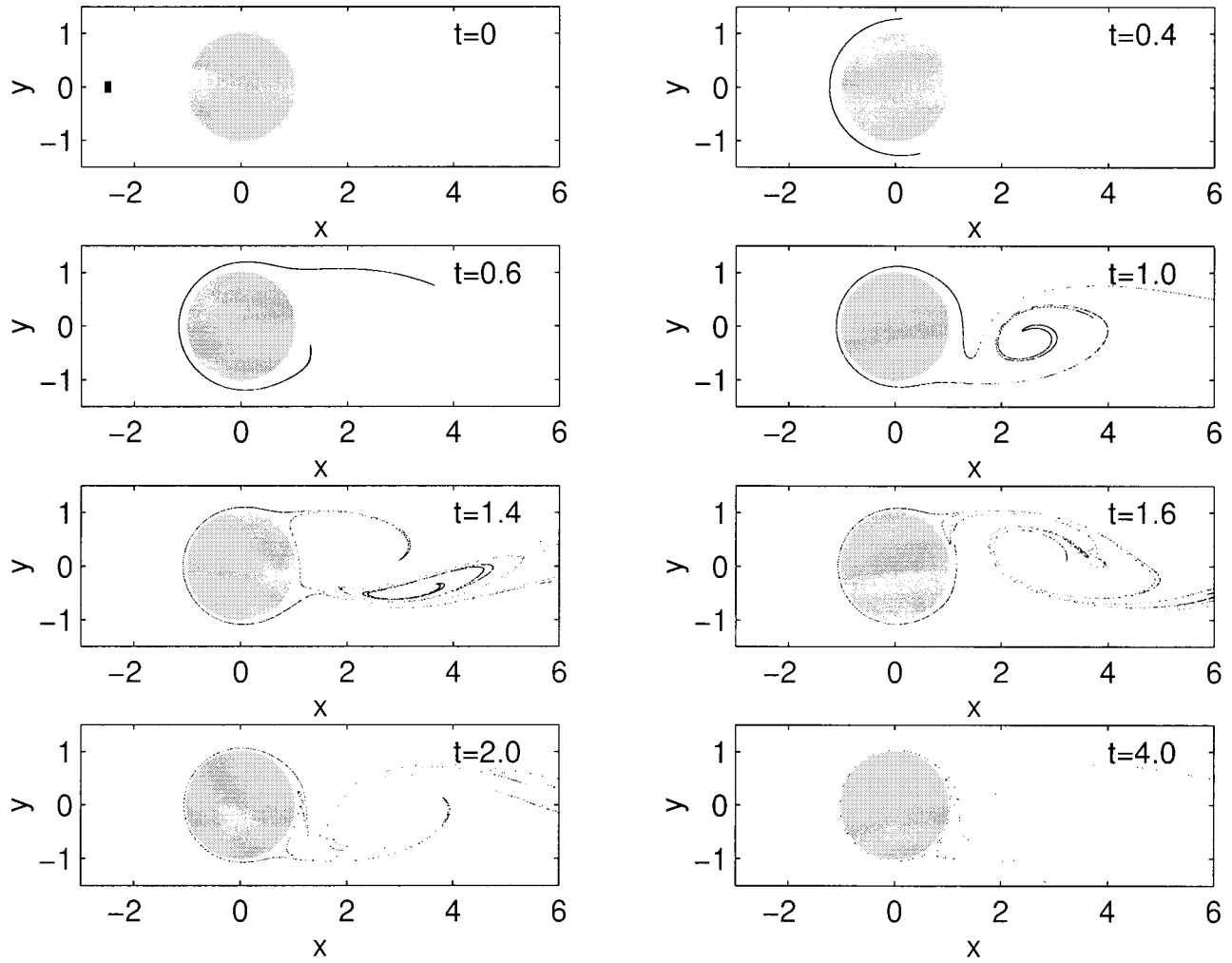Note that, although $\delta$ converges to a steady state, the material content does not. There is a permanent *dilution* in

FIG. 2. The evolution of a droplet of passively advected tracers is shown at the time instances $t=0,\frac{2}{5},\frac{3}{5},1,\frac{7}{5},\frac{8}{5},2$, and 4. The initial droplet is a rectangle of linear size $0.1\times0.2$, in $x$ and $y$ directions, respectively, and it is centered around $x=-2.5$ and $y=0$. It contains 20 000 particles. Note that the pattern traced out after a short transient is similar to the corresponding patterns of Fig. 1. The coverage of the unstable manifold by the tracers is not perfect due to the finite number of particles.

the covered region due to diffusion, and since the number of colored particles decreases in the fixed region of observation as $\exp(-\kappa t)$, their concentration also decreases with this rate asymptotically.

Next, it is worth contrasting the case of diffusion with that of nondiffusive passive advection in a *random* flow. By random we mean that the flow parameters $\mu$ entering the streamfunction $\psi$ are not constant in the course of time but fluctuate around their mean $\bar{\mu}$, i.e., $\mu(t)=\bar{\mu}+\delta\mu(t)$, where $\delta\mu(t)$ is the fluctuation. In our particular example of the flow around a cylinder, this can be realized either by letting the cylinder fluctuate randomly but slowly around its original center with some small amplitude, or, more naturally, by going to higher Reynolds numbers where the detachment of vortices is no longer strictly periodic, but rather modulated with a nonperiodic, chaotic component. Thus, the case of flows where the velocity field is changing *chaotically* in time can also be considered as a random flow. In any case the instantaneous streamlines are smooth, i.e., the flow is far from turbulent.

By considering snapshots of the passively advected par-

ticles with some sampling time $\tau$ (which can be completely independently chosen from the original period $T$ of the flow) one finds a map $M_{\mu_n}$ which connects the particle positions $(x_n,y_n)$ and $(x_{n+1},y_{n+1})$ on two subsequent snapshots in the form of

$$(x_{n+1},y_{n+1})=M_{\bar{\mu}+\delta\mu_n}(x_n,y_n).\tag{15}$$

Map (15) is area preserving. It further differs from (10) not only in the nonadditive character of the noise, but more importantly in the fact that *all* advected particles feel the *same* realization of the flow at a given instant of time, while the additive noise in (10) is considered to be independent for any particle. More generally, map (15) expresses the randomness of the velocity fields, i.e., randomness in the Eulerian picture, while map (10) describes stochasticity in the advection process, i.e., in the Lagrangian picture for exactly periodic flows. They are both extensions of map (3) for different types of random perturbations.

If the fluctuations of the parameters can be considered to be taken with a *stationary* probability distribution, i.e., if the

probability $P(\delta\mu)$ of the parameter fluctuations is time-($n$)-independent, then map $M_{\mu_n}$ is called a *random map*. Note that the particular form of the distribution $P(\delta\mu)$ (e.g., Gaussianity) does not need to be specified. The stationarity can be insured if the flow has some structural stability and if the observational time is sufficiently long. These criteria are met by the examples mentioned above.

The theory of random maps has been originally worked out in the context of dissipative systems,[40] and applied to flows in closed containers.[41] This approach has recently been extended to advection in open flows[42,43] which implies the use of open area-preserving random maps. We note, in passing, that if the condition of stationarity is not fulfilled, i.e., either structural stability of the flow, or long observational times are not available, the theory of random maps is not applicable. In such cases the advection dynamics is not chaotic, and hence beyond the scope of the present article; however, concepts of dynamical systems can usefully be applied to characterize such advection.[44]

The motion of individual particles in random maps is as ''random looking'' as that of diffusive particles. By considering however *ensembles* of particles which are in this case subjected to the same realization of the random flow, one can uniquely define chaos characteristics (like $\lambda$, $\kappa$, and $K_0$), which are to be treated as averages over all realizations (or over sufficiently long times). Perhaps even more surprisingly, tracer patterns converge towards *fractal* objects, and the analogs of the chaotic saddle, as well as of its manifolds can be defined. Moreover, for the information dimension $D_1$ of the analog of the unstable manifold Eq. (4) turns out to remain valid.[42,43] Thus, for ensembles of nondiffusive tracers, the behavior is very similar to that in time periodic flows, and, in spite of the randomness, an exact fractal scaling holds *without* any lower cutoff due to noise. [Note that for ensembles of diffusive tracers described by map (10) the fractality of droplet patterns is washed out below the cutoff scales (12) or (13).] It is worth mentioning that advection by random flows, especially by chaotically moving point vortices,[43] is reminiscent to advection by two-dimensional turbulence,[45] at least on finite time scales.

## III. CHEMICAL ACTIVITY

We showed in the previous sections that the fractal unstable manifold is the avenue of long-time propagation and transport of passive tracers in open flows. It is natural to expect that this object also plays a central role if the tracers are chemically active and can react with other tracers or with the background flow. The problem of chemical reactions in imperfectly mixed flows attracts ongoing interest[46,47] and has important applications to environmental chemistry.[48]

For our discussion let us assume that the activity of the advected particles is some kind of ''infection'' leading to a change of properties if particles come close enough to each other. Particles with new properties are the products. For nondiffusive tracers, an *enhancement* of activity can be observed around the chaotic saddle and its unstable manifold since it is there where the active tracers spend the longest time close to each other. Then, as the products are passively

advected, they trace out the unstable manifold. (The enhancement of activity is meant in comparison with nonchaotic, i.e., stationary flows.)

To be specific, we consider a simple *kinetic* model[49] where two passively advected particles of different kind undergo a reaction if and only if they come within a distance $\sigma$. The distance $\sigma$ is called the *reaction range*, and, as we see later, can also be considered as a diffusion distance. We study (cf. Refs. 50 and 51) an auto-catalytic process $A+B \rightarrow 2B$ in which component $A$ is the background material covering the majority of the entire fluid surface. For computational simplicity we assume that the reactions are instantaneous and take place at integer multiples of a time lag $\tau$. Thus, $\sigma$ and $\tau$ are the two new parameters characterizing the chemical process.

Figure 3 displays the results of a numerical simulation showing the spreading of a small droplet of $B$ (black) in the course of time. The background is considered to be covered by $A$ (white). Note the rapid increase of the $B$ area and the formation of a filamental structure. After about four periods, the chemical reaction takes on the period of the flow and reaches a *steady state*. In this steady state, the reaction products are apparently distributed in strips of finite width along the unstable manifold, and the $B$ particles trace out a stationary pattern on a stroboscopic map taken with the period $T$ of the flow. On linear scales larger than an average width $\epsilon^*$ the $B$ distribution is a fractal of the *same* dimension $D_0$ or $D_1$ as the unstable manifold of the reaction-free flow.

Next we present a simple theory, a slightly extended version of the one given in Refs. 50 and 51 (where the unstable manifold was assumed to be a monofractal with $D_0 = D_1$). The basic observation is that after a sufficiently long time, the filaments of the unstable manifold will be covered in narrow strips by material $B$ due to its autocatalytic production. The product is distributed on a fattened-up unstable manifold. Let $\varepsilon_n$ denote the average width of these strips right before reaction takes place. The effect of the reaction is then a broadening of the width by an amount proportional to the reaction range $\sigma$: $\varepsilon_n \rightarrow \varepsilon_n + c\sigma$. Here $c$ is a dimensionless number expressing geometrical effects. It turns out to be slightly time dependent, but for simplicity we consider it to be constant in what follows. In the next period of length $\tau$ there is no reaction, just contraction towards the unstable manifold. Therefore, the width $\varepsilon_{n+1}$ right before the next reaction can be given as

$$\varepsilon_{n+1} = (\varepsilon_n + c\sigma)e^{-\lambda\tau}. \tag{16}$$

This is a recursive map, for the actual width of the $B$-strips on snapshots taken with multiples of the time lag $\tau$. Its solution converges to the fixed point

$$\varepsilon^* = \frac{c\sigma}{e^{\lambda\tau} - 1}. \tag{17}$$

In the time-continuous limit $\tau \rightarrow 0$, $\sigma \rightarrow 0$, but keeping $\sigma/\tau \equiv v_r$ constant, one obtains the differential equation:

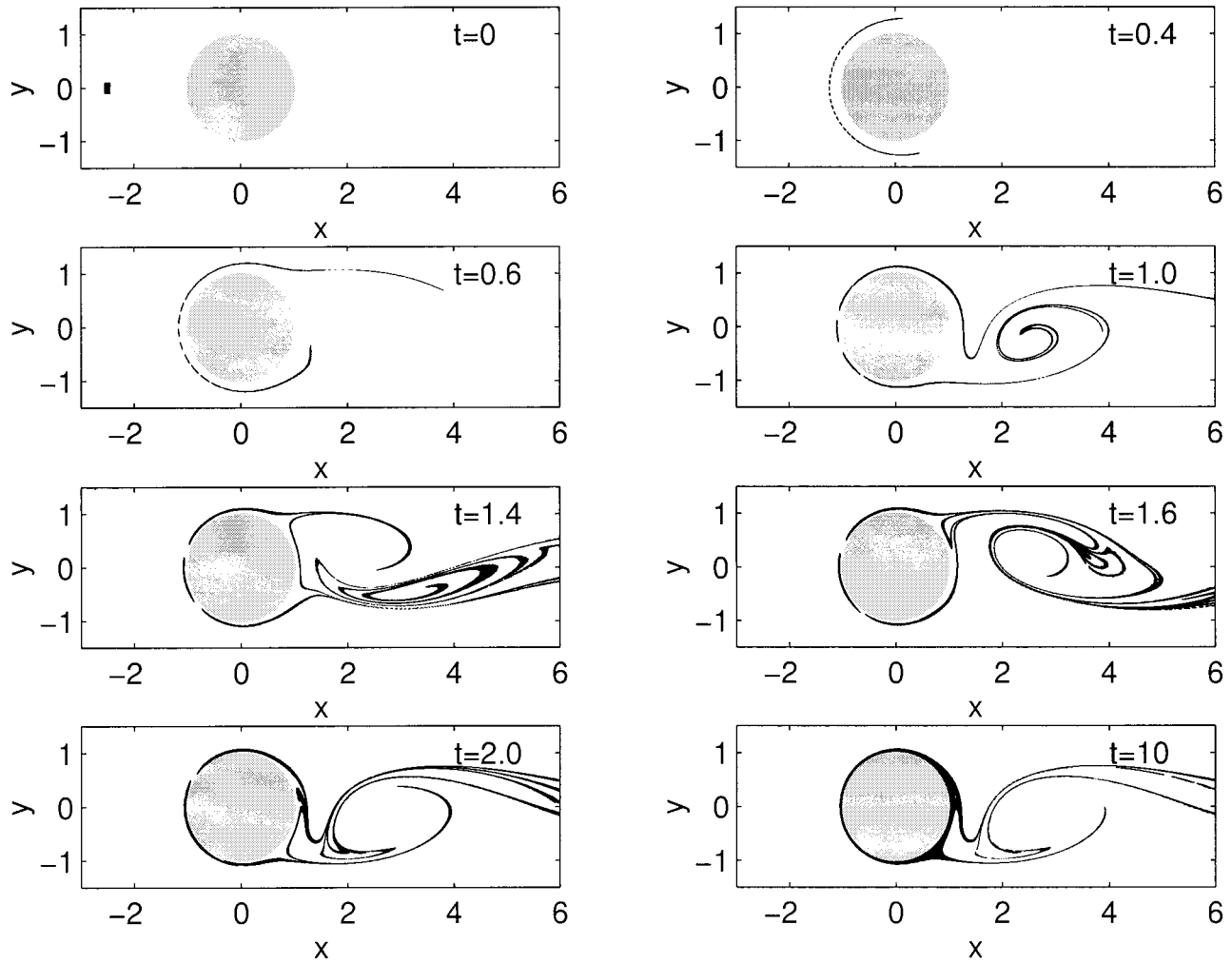$$\dot{\varepsilon} = cv_r - \lambda\varepsilon. \tag{18}$$

FIG. 3. Time evolution of autocatalytic tracers is shown at the time instances $t = 0, \frac{2}{5}, \frac{3}{5}, 1, \frac{7}{5}, \frac{8}{5}, 2$, and 10. The initial droplet is the same as in Fig. 2. The pattern traced out after reaching the stationary state is a fattened-up copy of the unstable manifold, which is the skeleton of activity. The chemical model parameters are $\sigma = 0.005$ and $\tau = 0.2$. The simulation was performed on a rectangular grid of size 0.005.

Here $v_r$ can be interpreted as a reaction velocity. The reaction is tending to broaden the width, while convergence towards the unstable manifold produces shrinking. These two effects are competing, and when compensating each other, they lead to the steady solution

$$\varepsilon^* = \frac{c v_r}{\lambda}. \tag{19}$$

At this point, it is worth making a comparison to the effect of diffusion in reaction-free flows. Both reaction and diffusion lead to a broadening, expressed in the similarity between Eqs. (11) and (16), (14) and (18), and also between the steady state results (12) and (17), (13) and (19). The latter suggest the correspondence $D \leftrightarrow \sigma^2/\tau$ in the discrete time version, and $D \leftrightarrow v_r^2/\lambda$ in the continuous time limit. This implies that the reaction range or reaction velocity plays a similar role as diffusion in reaction free flows. Note, however, that in contrast to the latter case, there is *no dilution* in the chemical model due to the reaction.

An important consequence of the $\varepsilon$-dynamics is the time evolution of the area $\mathcal{A}_B$ occupied by particles $B$ in a fixed region of observation. This area scales as $\mathcal{A}_B \approx \epsilon^{2-D_1}$ with

$D_1$ as the information dimension of the unstable manifold [cf. the derivation of (4)] for any box size $\epsilon$ not shorter than the width $\varepsilon$ of the $B$-strips. We can thus choose $\epsilon = \varepsilon \approx \mathcal{A}_B^{(1/(2-D_1))}$, and rewrite (18) so that it represents an equation for the area:

$$\dot{\mathcal{A}}_B = -\kappa \mathcal{A}_B + c \frac{\kappa v_r}{\lambda} \mathcal{A}_B^{-\beta}. \tag{20}$$

Here

$$\beta \equiv (D_1 - 1)/(2 - D_1) = \frac{\lambda - \kappa}{\kappa} = \frac{K_1}{\kappa} \tag{21}$$

is a nontrivial exponent. Since the manifold's dimension lies between 1 and 2, and $K_1 > 0$, the exponent $\beta$ is typically positive. For $D_0 = D_1 = 1$ the differential equation (20) describes a classical surface reaction along a line with front velocity $v_r$ in the presence of escape. For $1 < D_1 < 2$ it represents a novel form of reaction equations containing also a negative power of concentration due to the fractality of the unstable manifold. Such processes are generalizations of classical surface reactions.[33] The enhancing reaction term

with a *negative* power of the area occupied by $B$ is due to the fractality of the unstable manifold. The less $B$ material is present, the more effective the reaction is, because the resolved perimeter is larger. Thus the manifold effectively increases the free surface area where the reaction takes place and thus acts as a *catalyst*.

Let us finally sketch how the effect of molecular diffusion would modify the results. In such a case one expects the combination of (14) and (18) to hold, i.e., the differential equation

$$\dot{\varepsilon} = c v_r + \frac{D}{\varepsilon} - \lambda \varepsilon \tag{22}$$

for the width of the $B$-strip covering the unstable manifold. Here $D$ is the molecular diffusion coefficient. This equation also possesses a steady-state solution with a constant $\varepsilon^*$. Around this state the solution is similar to that of (18) with an *effective reaction velocity*

$$v_{r,\text{eff}} = v_r + \frac{D}{c \varepsilon^*}. \tag{23}$$

Thus close to the steady state, the inclusion of diffusion only renormalizes the effect of the reaction velocity.

Alternatively, one can also consider the stochastic version of (18) by adding a Gaussian white noise term $\xi$ with autocorrelation strength $2D$ to the right-hand side. The same derivation which led to (20) then yields (see also Ref. 51)

$$\dot{\mathcal{A}}_B = -\kappa \mathcal{A}_B + \frac{\kappa}{\lambda} \mathcal{A}_B^{-\beta} (c v_r + \xi), \tag{24}$$

which is a nonlinear Langevin-type equation with multiplicative noise. This indicates that on the macroscopic level, for the total area of $B$, the noise appears in a nontrivial fashion, and its effect is enhanced by fractality via the prefactor $\mathcal{A}_B^{-\beta}$.

## IV. BIOLOGICAL ACTIVITY

Our discussion on chemical reaction in open flows can be naturally extended to population dynamics models provided the species' advection can be approximated with the passive tracer model. In such cases, we expect that different species accumulate along the unstable manifold of the passive advection problem. Here we consider a particular problem of several different species competing for the same resource. According to the classical theory, the number of coexisting species can at most be equal to the number of independent resources, if the environment is well stirred and homogeneous.[52] It is well known that in plankton communities the number of coexisting species can be much larger than that of the resources. In the wake of an obstacle we expect that several species can coexist in spite of competing for a single resource. This would be again a deviation from classical results due to the fractality of the unstable manifold. In fact, our model[53] may also shed some new light on this apparent contradiction between empirical and theoretical studies, sometimes called the ''plankton paradox.''[52]

Our competition dynamics for a single background material $A$ is a simple model of replication and competition with point like particles (species) of type $B$ and $C$. There is a constant inflow of material $A$ into the system on the entire surface of the flow. Species $B$ ($C$) catalyzed by material $A$ reproduce instantaneously at time intervals $\tau$ only if their centers come within a distance $\sigma_B$ ($\sigma_C$) to particles of type $A$. Due to the open character of the flow, the particles will be drifted downstream, therefore leaving the mixing region of the wake with escape rate $\kappa$. In addition, there is a spontaneous decay of individuals to $A$ with mortality rates $\delta_B$ and $\delta_C$. Two autocatalytic processes $A + B \to^{\gamma_B} 2B$, $B \to^{\delta_B} A$ and $A + C \to^{\gamma_C} 2C$, $C \to^{\delta_C} A$ describe thus replication and competition. Material $A$ is the common limiting resource for both species $B$ and $C$.

In our numerical experiment, we place two droplets of organisms from species $B$ and $C$ into the flow in front of the cylinder. We find that both species $B$ and $C$ are pulled onto the unstable manifold of the chaotic set, as their initial positions overlap with its stable manifold. Thus, both species $B$ and $C$ are trapped in the wake, and are accumulated along the filaments of the fractal unstable manifold. This leads to an enhancement of their activity, with both of them having increased access to the background $A$ for which they compete. Along the fractal unstable manifold, $B$ and $C$ can be separated quite efficiently by filaments of $A$. Due to the imperfect mixing, the competition is reduced by spatial separation and the survival is catalyzed by increased access to material $A$. This leads to the coexistence of the competing species for a wide range of parameter values.

Figure 4 shows a series of snapshots of the organisms in the region of observation from the insertion of the droplets at time $t=0$ to time $t=20$. The filamental structure shown in Fig. 4 is reminiscent of the patterns found in mesoscale plankton models.[54–58]

Note that in the asymptotic state species $B$ covers the surface of the cylinder, while species $C$ occupies mainly the wake. This shows that the actual number of individuals does not only depend on the parameters but also on the initial conditions. The mere fact of coexistence is, however, independent of these in a broad range.

## V. CONCLUDING REMARKS

Finally we summarize those features of the chemical and biological activity which we believe are generally valid in typical open flows.

(i)    Active processes take place around the unstable manifold of the passive advection's saddle. If the passive advection is chaotic, the manifold is a fractal and consequently active processes also lead to fractal patterns.

(ii)    Although the fractal manifold is of measure zero, due to the chemical reaction (or population dynamics) the amount of active tracers covering this manifold is finite. This implies that the fractality can be observed on length scales larger than the average width of the fattened-up manifold.

(iii)    On one hand, the fractal skeleton results in an increase of the active surface and acts as a catalyst for
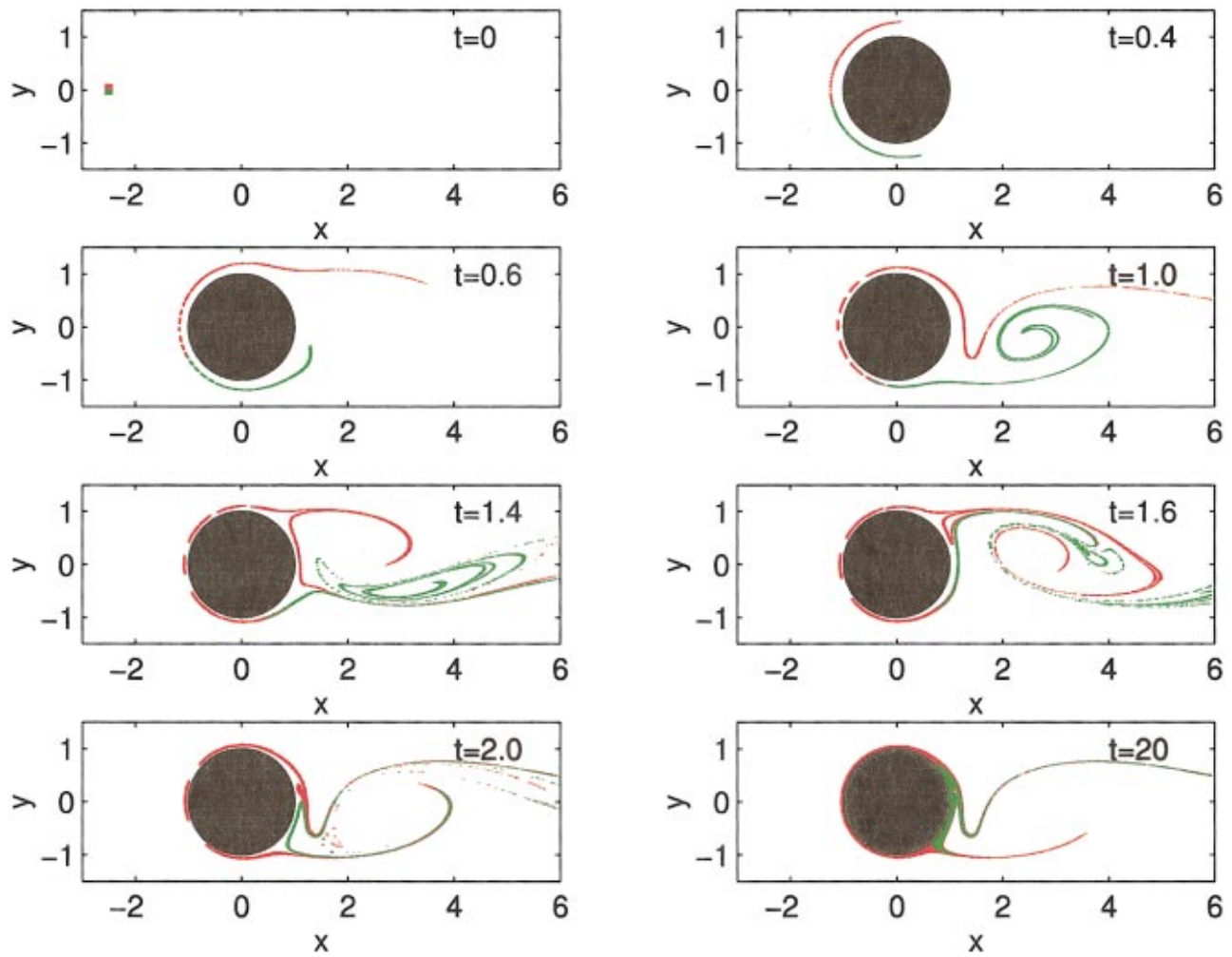
FIG. 4. (Color) Time evolution of two competing species is shown at time instances $t=0, \frac{2}{5}, \frac{3}{5}, 1, \frac{7}{5}, \frac{8}{5}, 2$, and 20. The initial position of species $B$ (green) and $C$ (red) is a square of linear size 0.1 centered around $x=-2.5$, $y=-0.05$ and $y=0.05$, respectively. The initially small droplets of species $B$ and $C$ are eventually pulled along the unstable manifold. The stationary state is reached after a short time: the last two snapshots (taken at $t=2$ and $t=20$) are almost the same. Species $C$ (red) occupies also the boundary layer around the cylinder, while $B$ (green) is trapped mainly on the chaotic set in the wake. The model parameters are $\sigma_B=\frac{1}{150}$, $\sigma_C=\frac{1}{300}$, $\delta_B=0.5$, $\delta_C=0.0001$, and $\tau=\frac{1}{5}$. The simulation was performed on a rectangular grid of size 0.001.

the growth process. On the other hand, different species are separated efficiently along the fractal manifold decreasing competition.

(iv)    The derivation of reaction (or population dynamics) equations is similar to that of the macroscopic transport equations from microscopic molecular dynamics. The presence of the ever-refining fractal structures generates new terms in the macroscopic equations, leading to interesting new effects like singular source term in the reaction equation.

(v)    The macroscopic equations describing the active process typically reach a steady state synchronized with the background flow's temporal behavior. If more than one species is present, coexistence is typical in the steady state for a wide range of parameter values.

We emphasize that our method of studying activity in open flows is based on a fully *deterministic* approach of passive advection. It is described by means of *ordinary* differential equations. Nevertheless, we are able to study complex

*spatial patterns* which is due to the fact that the phase space of Eqs. (1) and (2) coincides with the geometrical space (the only example of this sort to our knowledge). In order to see these spatial patterns we use *ensembles* of particles, corresponding to droplets in the hydrodynamical context. As pointed out here, even effects similar to that of diffusion can be described by the inclusion of an interaction range or reaction velocity. In this approach Lagrangian characteristics, like Lyapunov exponents, entropies, and dimensions seem to be natural parameters of the processes. It is of interest to see how this approach is related to the more traditional one based on *partial* differential equations describing reaction-advection-diffusion effects, and carrying Eulerian parameters like shears or diffusion (see e.g., Refs. 46, 48, and 56–59). This problem clearly needs further investigation.

## ACKNOWLEDGMENTS

[1] J. M. Ottino, *The Kinematics of Mixing: Stretching, Chaos and Transport* (Cambridge U. P., Cambridge, 1989).

[2] L. Yu, C. Grebogi, and E. Ott, in *Nonlinear Structures in Physical Systems* (Springer-Verlag, New York, 1990), pp. 223–231.

[3] A. Crisanti, M. Falcioni, G. Paladin, and A. Vulpiani, Riv. Nuovo Cimento **14**, 207 (1991).

[4] H. Aref (ed.) *Chaos Applied to Fluid Mixing*, special issue, Chaos Solitons and Fractals **4**, 745–1116 (1994).

[5] J. B. Kadtke and E. A. Novikov, Chaos **3**, 543 (1993).

[6] R. B. Rybka *et al.*, Phys. Rev. E **48**, 757 (1993).

[7] T. H. Solomon and J. P. Gollub, Phys. Rev. A **38**, 6280 (1988); T. H. Solomon, E. R. Weeks, and H. L. Swinney, Physica D **76**, 70 (1994).

[8] R. T. Pierrehumbert, Chaos, Solitons and Fractals **4**, 1091 (1994).

[9] V. V. Meleshko and G. J. F. van Heijst, Chaos, Solitons and Fractals **4**, 977 (1994); V. V. Meleshko *et al.*, Phys. Fluids A **4**, 2779 (1992).

[10] G. Boffetta, A. Celani, and P. Franzese, J. Phys. A **29**, 3749 (1996).

[11] Z. Neufeld and T. Tél, J. Phys. A **30**, 2263 (1997).

[12] J. B. Weiss, A. Provenzale, and J. C. McWilliams, Phys. Fluids **10**, 1929 (1998).

[13] M. Giona, Fractals **5**, 333 (1997); M. M. Alvarez *et al.*, Phys. Rev. Lett. **81**, 3395 (1998); M. Giona and A. Adrover, *ibid*. **81**, 3864 (1998); M. Giona *et al.*, Physica D **132**, 298 (1999); A. Adrover and M. Giona, Phys. Rev. E **60**, 347 (1999).

[14] L. Kuznetsov and G. Zaslavsky, Phys. Rev. E **58**, 7330 (1998); ''Passive particle transport in three-vortex flows,'' Phys Rev. E (in press).

[15] A. Provenzale, Annu. Rev. Fluid Mech. **31**, 55 (1999).

[16] A. Babiano, J. H. E. Cartwright, O. Piro, and A. Provenzale, preprint, 1999.

[17] V. Rom-Kedar and A. C. Poje, Phys. Fluids **11**, 2044 (1999).

[18] S. Jones and H. Aref, Phys. Fluids **31**, 469 (1988).

[19] K. Shariff, A. Leonard, N. J. Zabusky, and J. H. Ferziger, Fluid Dyn. Res. **3**, 337 (1988).

[20] V. Rom-Kedar, A. Leonard, and S. Wiggins, J. Fluid Mech. **214**, 347 (1990).

[21] K. Shariff, T. H. Pulliam, and J. M. Ottino, Lect. Appl. Math. **28**, 613 (1991).

[22] K. Shariff and A. Leonard, Annu. Rev. Fluid Mech. **24**, 235 (1992).

[23] C. Jung and E. Ziemniak, J. Phys. A **25**, 3929 (1992).

[24] C. Jung, T. Tél, and E. Ziemniak, Chaos **3**, 555 (1993).

[25] E. Ziemniak, C. Jung, and T. Tél, Physica D **76**, 123 (1994).

[26] Á. Péntek, T. Tél, and Z. Toroczkai, J. Phys. A **28**, 2191 (1995); Fractals **3**, 33 (1995); Int. J. Bifurcation Chaos Appl. Sci. Eng. **6**, 2619 (1996).

[27] Á. Péntek, Z. Toroczkai, T. Tél, C. Grebogi, and J. A. Yorke, Phys. Rev. E **51**, 4076 (1995).

[28] G. Stolovitzky, T. J. Kaper, and L. Sirovich, Chaos **5**, 671 (1995).

[29] J. A. Kennedy and J. A. Yorke, Topology Appl. **80**, 201 (1997).

[30] M. A. F. Sanjuan *et al.*, Chaos **7**, 125 (1997); Phys. Rev. Lett. **78**, 1892 (1997); J. Kennedy *et al.*, Topol. Appl. **94**, 207 (1999); F. Duan and S. Wiggins, Nonlinear Processes Geophys **4**, 125 (1997).

[31] G. Károlyi and T. Tél, Phys. Rep. **290**, 125 (1997).

[32] Z. Toroczkai, G. Károlyi, Á. Péntek, T. Tél, C. Grebogi, and J. A. Yorke, Physica A **239**, 235 (1997).

[33] L. D. Landau and E. M. Lifschitz, *Fluid Mechanics*, Vol. 6 of *Course of Theoretical Physics*, 2nd ed. (Pergamon, Oxford, 1987).

[34] T. Tél, in *Directions in Chaos*, Vol. 3, edited by H. Bai-lin (World Scientific, Singapore, 1990), pp. 149–211; in *STATPHYS'19*, edited by H. Bai-lin (World Scientific, Singapore, 1996), pp. 346–362; E. Ott, *Chaos in Dynamical Systems* (Cambridge U.P., Cambridge, 1993).

[35] M. Van Dyke, *An Album of Fluid Motion* (Parabolic, Stanford, 1982).

[36] H. Kantz and P. Grassberger, Physica D **17**, 75 (1985).

[37] G. H. Hsu, E. Ott, and C. Grebogi, Phys. Lett. A **127**, 199 (1988).

[38] S. Newhouse and T. Pignataro, J. Stat. Phys. **72**, 1331 (1993).

[39] J. C. Sommerer, H.-C. Ku, and H. E. Gilreath, Phys. Rev. Lett. **77**, 5055 (1996).

[40] E. Romeiras, C. Grebogi, and E. Ott, Phys. Rev. A **41**, 784 (1990).

[41] L. Yu, E. Ott, and Q. Chen, Physica D **53**, 102 (1991); J. C. Sommerer and E. Ott, Science **259**, 281 (1993); C. Reyl, T. Antonsen, and E. Ott, Physica D **111**, 202 (1998).

[42] J. Jacobs, E. Ott, T. Antonsen, and J. Yorke, Physica D **110**, 1 (1997).

[43] Z. Neufeld and T. Tél, Phys. Rev. E **57**, 2832 (1998).

[44] P. D. Miller, C. K. R. T. Jones, A. M. Rogerson, and L. J. Pratt, Physica D **110**, 105 (1997); G. Haller and A. C. Poje, *ibid*. **119**, 352 (1998); A. C. Poje and G. Haller, J. Phys. Oceanogr. **29**, 1649 (1999); A. C. Poje, G. Haller, and I. Mezić, Phys. Fluids **11**, 2963 (1999).

[45] D. Elhmaidi, D. A. Provenzale, and A. Babiano, J. Fluid Mech. **257**, 533 (1993); A. Babiano, G. Boffetta, A. Provenzale, and A. Vulpiani, Phys. Fluids **6**, 2465 (1994); A. Provenzale, A. Babiano, and B. Villone, Chaos, Solitons and Fractals **5**, 2055 (1995).

[46] Z. Neufeld, C. López, and P. H. Haynes, Phys. Rev. Lett. **82**, 2606 (1999).

[47] H. Lustfeld and Z. Neufeld, J. Phys. A **32**, 3717 (1999).

[48] S. Edouard, B. Legras, B. Lefevre, and R. Eymard, Nature (London) **384**, 444 (1996).

[49] G. Metcalfe and J. M. Ottino, Phys. Rev. Lett. **72**, 2875 (1994); Chaos, Solitons and Fractals **6**, 425 (1995).

[50] T. Toroczkai, G. Károlyi, Á. Péntek, T. Tél, and C. Grebogi, Phys. Rev. Lett. **80**, 500 (1998).

[51] G. Károlyi, Á. Péntek, Z. Toroczkai, T. Tél, and C. Grebogi, Phys. Rev. E **59**, 5468 (1999).

[52] W. S. C. Gurney and R. N. Nisbet, *Ecological Dynamics* (Oxford U. P., Oxford, 1998).

[53] I. Scheuring, G. Károlyi, Á, Péntek, T. Tél, and Z. Toroczkai, ''A model for resolving the plankton paradox: Coexistence in open flows,'' Freshwater Biology (in press).

[54] E. R. Abraham, Nature (London) **391**, 577 (1998).

[55] J. Arístegui, P. Tett, A. Hernández-Guerra, G. Basterretxea, M. F. Montero, K. Wild, P. Sangrá, S. Hernández-León, M. Cantón, J. A. García-Braun, M. Pacheco, and E. D. Barton, Deep-Sea Res. **44**, 71–96 (1997).

[56] S. A. Spall and K. J. Richards, ''A numerical model of mesoscale frontal instabilities and plankton dynamics,'' Deep-Sea Res. (in press).

[57] C. López, Z. Neufeld, E. Hernandes-Garcia, and P. H. Haynes, ''Chaotic advection of reacting substances: Plankton dynamics on a meandering jet,'' submitted to Phys. Chem. Earth (1999).

[58] A. P. Martin, ''On filament width in oceanic plankton distribution,'' submitted to J. Plankton Res. (1999).

[59] P. H. Haynes, in *Mixing: Chaos and Turbulence*, edited by H. Chate and E. Villermaux (Kluwer, Dordrecht, 1999).